



# Adaptive Neuro Fuzzy Inference System Least-Mean-Square-Based Control Algorithm for DSTATCOM

P PAVANI,

M.Tech, TUDI NARASIMHA REDDY INSTITUTE OF TECHNOLOGY & SCIENCES, GUDUR,  
BIBINAGAR, YADADRIBHONGIRI, TELANGANA

Mr. P NIRANJAN,

Assistant professor, TUDI NARASIMHA REDDY INSTITUTE OF TECHNOLOGY & SCIENCES, GUDUR,  
BIBINAGAR, YADADRIBHONGIRI, TELANGANA

**Abstract:** This paper proposes the continuous execution of a three-phase distribution static compensator (DSTATCOM) utilizing adaptive neuro fuzzy inference system least-mean-square (ANFIS-LMS)- based control calculation for pay of current-related power quality issues. This calculation is confirmed for different functions of DSTATCOM, for example, harmonics remuneration, power factor redress, load adjusting, and voltage regulation. The ANFIS-LMS-based control calculation is utilized for the extraction of fundamental active and reactive power components from nonsinusoidal load currents to appraise reference supply currents. Constant approval of the proposed control calculation is performed on a created research center model of a shunt compensator. The constant execution of shunt compensator with ANFIS-LMS-based control calculation is discovered satisfactory under steady-state and dynamic load conditions. The execution of the proposed control calculation is likewise contrasted and settled step LMS and variable-step LMS (VSLMS) to exhibit its improved execution.

**Index Terms**— Adaptive filtering, adaptive neuro fuzzy inference system (ANFIS), harmonics cJTGomensation, power quality, unity power factor, voltage regulation.

## I. INTRODUCTION

THERE IS an expanded penetration of power electronics-based loads in businesses and local part which infuse harmonics in the distribution system. Moreover, poor power factor, load unbalancing, and high nonpartisan current are some of the power quality issues presented by an assortment of loads in, the distribution system. Power quality issues, for example, waveform distortion are because of harmonics and load unbalancing, which cause unfortunate weight on the distribution system. Numerous topologies have been created for remuneration of power quality

issues which incorporate the use of passive filters, active filters, and hybrid filters. Active power filter devices are utilized for stifling the impacts of nonsinusoidal load current, directing the distribution bus voltage, wiping out the impact of poor power factor, and accomplishing adjusted supply currents even under uneven load conditions. The active filters are otherwise called distribution static compensator (DSTATCOM). A DSTATCOM is regularly a voltage source converter (VSC) - based shunt compensator [1] – [3]. The execution and control of DSTATCOM have turned out to be conceivable because of progression in advanced signal processors (DSPs) and self-commutating semiconductor devices [4]– [6]. An improvement in power quality is accounted for utilizing a few new control systems.

An internal control of DSTATCOM is an essential to accomplish wanted execution in steady-state and dynamic conditions. Diverse procedures for extricating harmonics from contorted load current have been recommended by different creators. Instantaneous reactive power theory is based on the count of active and reactive powers by changing over three-phase voltages and currents into two phases. Christo Ananth et al.[7] discussed about E-plane and H-plane patterns which forms the basis of Microwave Engineering principles. This control system does not function admirably under nonsinusoidal supply voltages [8]. Synchronous reference outline theory [9] is based on the transformation of three-phase quantities into their dc partners, and low-pass filters (LPFs) are acknowledged for harmonic filtering[10], [11]. It is hard to evaluate the ideal parameters of these LPFs with hysteresis current controller. Some different calculations for removing the reference currents

have been created and successfully actualized. These incorporate instantaneous model reference adaptive control [12], single-phase active-reactive power theory [13], programming phase bolt circle (PLL)- based reference extraction [14], understood shut circle current control, and resounding controller [15]. Adaptive filtering [16], [17] has additionally been perceived as powerful control procedure for separating reference sinusoidal current from contorted load current. The benefit of adaptive filtering control methods is that they display better reaction under transient conditions. Various adaptive filtering calculations are accounted for and have discovered application in charge, correspondence, and signal handling. A few creators have proposed calculations based on least mean square (LMS) [18], variable least mean square (VLMS) adaptive filtering in charge system and signal preparing [19], [20], fuzzy inference-based variable-step LMS (VSLMS) [21], block least mean square calculation [22], artificial neural system (ANN)- based adaptive control [23], [24], and robust adaptive control procedure [25]. In this paper, an adaptive LMS calculation is created in which the step size parameters are refreshed utilizing adaptive neuro fuzzy inference system (ANFIS). An adaptive neuro fuzzy inference system least mean square (ANFIS-LMS)- based control calculation is created utilizing MATLAB/Simulink, what's more, its viability is tentatively checked. The extraction of sinusoidal reference current from misshaped load current is accomplished by controller activity. The proposed calculation is contrasted and settled step LMS and variable-step-based VSLMS as recommended in [18] – [20].

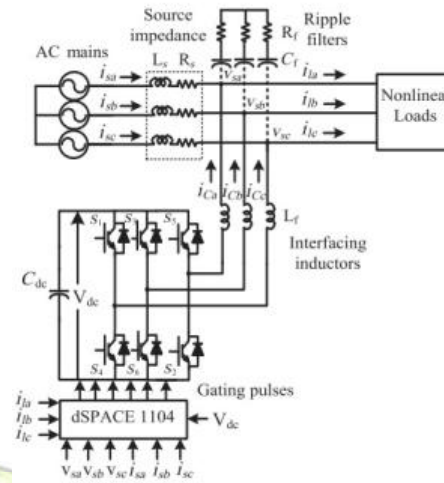


Fig. 1: System configuration of shunt compensator.

A noteworthy favorable position of the proposed control calculation is that it displays less static error and accomplishes quick joining. The step size evaluated utilizing ANFIS adapts quicker and accomplishes less static error in fundamental weight estimation. The proposed control calculation is utilized for the control of the shunt compensator and can enhance different parts of power quality, for example, harmonics remuneration, voltage regulation, power factor revision (PFC), and load adjusting. An improved execution is accomplished under steady state and in addition dynamic load conditions with the ANFIS-LMS-based adaptive system.

## II. SYSTEM CONFIGURATION

Fig. 1 demonstrates the schematic diagram of a three-phase shunt compensator. An utility supply of three-phase, 415 V and 50 Hz sustains the load. Little line impedance ( $L_s - R_s$ ) related with utility goes about as a feeder. The fundamental building block in the DSTATCOM is a VSC, which is demonstrated utilizing an all inclusive bridge in Simulink library. The VSC comprises of six protected door bipolar transistors (IGBTs) switches with hostile to parallel diodes. The nonlinear load is displayed utilizing uncontrolled rectifier with series R-L branch. The DSTATCOM is associated at PCC with the assistance of interfacing inductors ( $L_f$ ), used to filter compensator currents. High-switching frequency components created by IGBTs are wiped

out by resistive-capacitive (Rf – Cf) swell filters. Simulation investigation of the proposed system is influenced utilizing Sim To power System (SPS) toolbox in MATLAB/Simulink and the ongoing approval of the ANFISLMS-based control calculation is completed by building up a little scale model in the lab utilizing DSP controller.

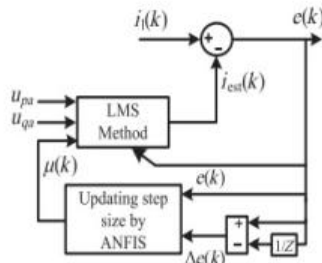


Fig.2: Error minimization by ANFIS-LMS

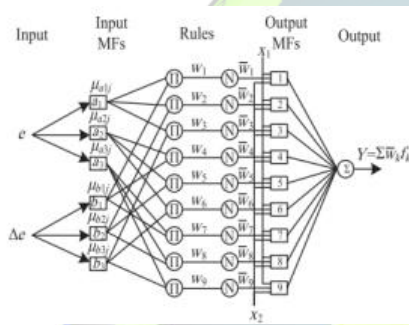


Fig.3: Structure of nine-rule ANFIS.

### III. CONTROL ALGORITHM

The definite portrayal of adaptive LMS procedure is introduced here, in which the step size parameter is refreshed utilizing ANFIS. An ANFIS LMS-based control calculation is created, and its mathematical detailing is presented. Both the LMS technique and ANFIS structure are appeared in Figs. 2 and 3, individually. The total block diagram of the control calculation is appeared in Fig. 4.

#### A. Estimation of Fundamental Active Power Components of Reference Supply Currents

Amplitude of PCC voltage ( $V_t$ ) is calculated as

$$V_t = \sqrt{2(v_{sa}^2 + v_{sb}^2 + v_{sc}^2)/3} \quad (1)$$

Where  $v_{sa}$ ,  $v_{sb}$ , and  $v_{sc}$  are the sensed PCC phase voltages.

In-phase unit templates of PCC voltages  $u_{pa}$ ,  $u_{pb}$ , and  $u_{pc}$  are derived as

$$u_{pa} = v_{sa}/V_t, u_{pb} = v_{sb}/V_t, \text{ and } u_{pc} = v_{sc}/V_t. \quad (2)$$

The difference ( $v_{de}$ ) between the sensed ( $V_{dc}$ ) and reference dc link voltage ( $V_{dc}^*$ ) is calculated and passed through a proportional integral (PI) controller. The output of the PI controller is an active power component, which is used to maintain dc link voltage at reference value and meets VSC losses. At  $k$ th sampling instant, the PI controller output is given as

$$w_{ploss}(k) = w_{loss}(k-1) + k_{pd}\{v_{de}(k) - v_{de}(k-1)\} + k_{id}(v_{de}(k)) \quad (3)$$

Where  $w_{ploss}$ ,  $k_{pd}$ , and  $k_{id}$  are PI controller output, proportional gain, and integral gain, respectively.

The nonsinusoidal load current is expressed at  $k$ th sampling instant as

$$i_l(k) = I_{lf} \sin(\omega k + \theta_f) + \sum_{h=5,7,\dots}^{\infty} I_{lh} \sin(h\omega k + \theta_h) \\ = i_{lf}(k) + i_{lh}(k) \quad (4)$$

Where  $I_{lf}$  and  $I_{lh}$  represent peak value corresponding to fundamental component and harmonic component of load current, respectively. Angles  $\theta_f$  and  $\theta_h$  represent phase angles of fundamental and harmonic components of load current, respectively.

The current corresponding to fundamental and harmonic components of load current can be further divided as

$$i_{lf}(k) = I_{lf} \sin \omega k \cos \theta_f + I_{lf} \cos \omega k \sin \theta_f \quad (5)$$

$$i_{lh}(k) = I_{lh} \sin h\omega k \cos \theta_f + I_{lh} \cos h\omega k \sin \theta_f. \quad (6)$$

Replacing  $I_{lf} \cos \theta_f$ ,  $I_{lf} \sin \theta_f$ ,  $I_{lh} \cos \theta_f$ , and  $I_{lh} \sin \theta_f$  by weights  $w_{a1}$ ,  $w_{b1}$ ,  $w_{ah}$ , and  $w_{bh}$ , respectively, the new equations are formed as

$$i_{lf}(k) = w_{a1} \sin \omega k + w_{b1} \cos \omega k \quad (7)$$

$$i_{lh}(k) = w_{ah} \sin h\omega k + w_{bh} \cos h\omega k \quad (8)$$

Where “ $h$ ” denotes the order of harmonics,  $h = 5, 7, \dots, \infty$ .



The estimated load current is computed from the optimum weights ( $w_{a1}$ ,  $w_{b1}$ ,  $w_{a5}$ , and  $w_{b5}$ ) expressed as

$$i_{\text{est}}(k) = \mathbf{W}^T \mathbf{X}(k) \quad (9)$$

Where the input vector  $\mathbf{X}(k)$  is given as  $\mathbf{X}(k) = [\sin\omega k, \cos\omega k, \sin 5\omega k, \cos 5\omega k, \dots]^T$ , which represents vector of unit in-phase and quadrature templates  $[u_{pa}, u_{qa}, u_{5pa}, u_{5qa}, \dots]^T$ . The unit quadrature templates are calculated in next section. The weight vector  $\mathbf{W}^T$  is represented as  $\mathbf{W}^T = [w_{a1}, w_{b1}, w_{a5}, w_{b5}, \dots]$ .

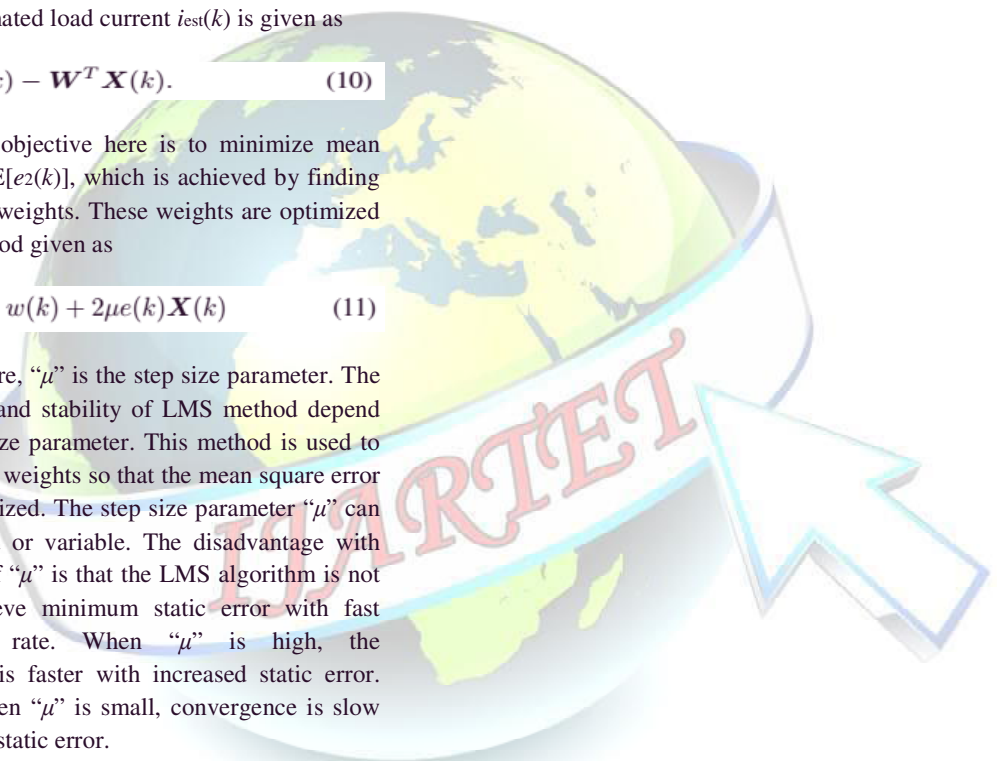
The error  $e(k)$ , between actual load current  $i_l(k)$  and estimated load current  $i_{\text{est}}(k)$  is given as

$$e(k) = i_l(k) - \mathbf{W}^T \mathbf{X}(k). \quad (10)$$

The objective here is to minimize mean square error  $E[e^2(k)]$ , which is achieved by finding the optimum weights. These weights are optimized by LMS method given as

$$w(k+1) = w(k) + 2\mu e(k)\mathbf{X}(k) \quad (11)$$

Where, " $\mu$ " is the step size parameter. The convergence and stability of LMS method depend on the step size parameter. This method is used to find optimum weights so that the mean square error can be minimized. The step size parameter " $\mu$ " can be kept fixed or variable. The disadvantage with fixed value of " $\mu$ " is that the LMS algorithm is not able to achieve minimum static error with fast convergence rate. When " $\mu$ " is high, the convergence is faster with increased static error. However, when " $\mu$ " is small, convergence is slow with reduced static error.



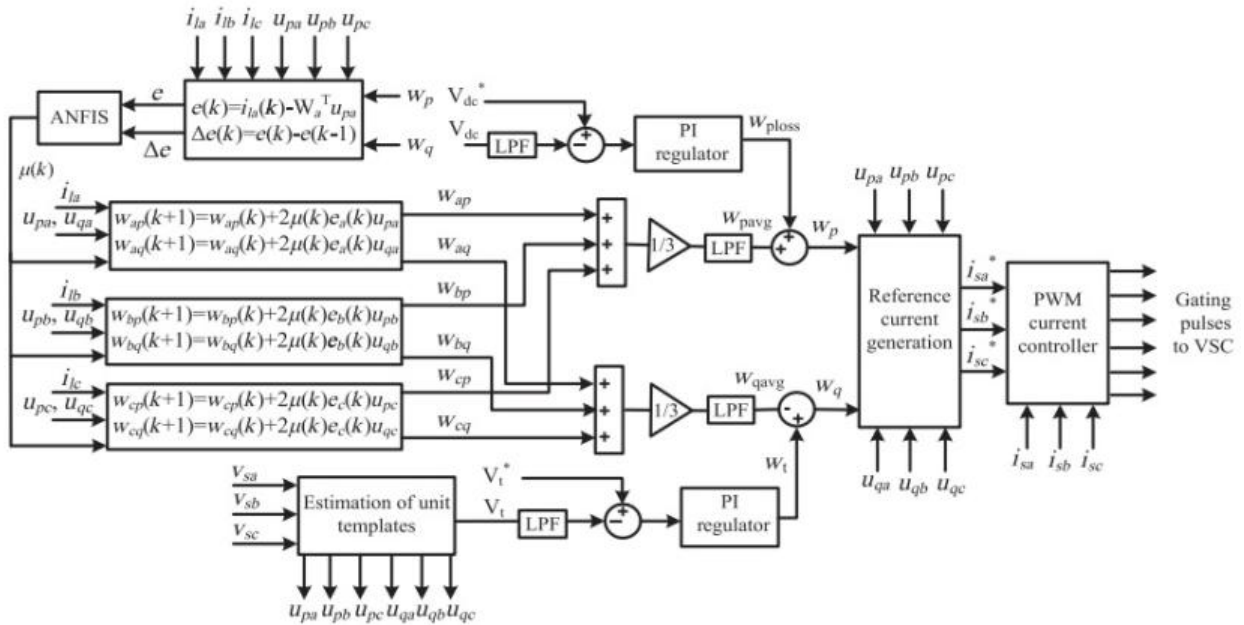


Fig.4: Block diagram of ANFIS-LMS-based control algorithm for DSTATCOM.

To solve the contradiction between the convergence rate and steady-state error, an ANFIS-based variation of step size “ $\mu$ ” is proposed in this paper. The structure of ANFIS is developed with two inputs, three membership functions (MFs), and nine rules as shown in Fig. 3. This represents both square and circular nodes, to identify different adaptive capabilities. The ANFIS structure uses first-order Sugeno-type fuzzy inference system [26], [27]. The function of each layer of ANFIS structure is given as follows.

*Layer 1:* This is the fuzzification layer, having two inputs. One input of this layer is error ( $x_1 = e(k)$ ) between actual and estimated values of load current ( $i_l(k) - W^T X(k)$ ), and other input is the change in error ( $x_2 = \Delta e(k)$ ). Each input function corresponds to three MFs, and the shape of MFs is represented as square bracket. The internal structure of each square bracket represents trapezoidal and triangular MFs. Equations related to each MF are given in Equations (12)-(14).

In those Equations from (12)-(14),  $\{m_i, n_i\}$  are set of parameters, and value of  $i = 1, 2, 3$ . The parameters  $\{m_i, n_i\}$  change with the change in value of error and correspondingly generate the linguistic

value of each MF. These parameters are known as premise parameters.

$$\mu_{a1}(x_1) = \mu_{b1}(x_2) = \begin{cases} 0, & x > m_1 \\ \frac{m_1 - x}{m_1 - n_1}, & n_1 \leq x \leq m_1 \\ 1, & x < n_1 \end{cases} \quad (12)$$

$$\mu_{a2}(x_1) = \mu_{b2}(x_2) = \begin{cases} 0, & x \leq m_1 \\ \frac{x - n_2}{p - n_2}, & n_2 < x \leq p \\ \frac{m_2 - x}{m_2 - p}, & p < x < m_2 \\ 0, & x \geq m_2 \end{cases} \quad (13)$$

$$\mu_{a3}(x_1) = \mu_{b3}(x_2) = \begin{cases} 0, & x < m_1 \\ \frac{x - m_3}{n_3 - m_3}, & m_3 \leq x \leq n_3 \\ 1, & x > n_3 \end{cases} \quad (14)$$

*Layer 2:* This layer is known as implication layer, and each node in this layer is fixed node. This layer represented as  $\Pi$ , and the output of each node of this layer is multiplication of its input signals

$$w_k = \mu_{a_{ij}}(x_1) \mu_{b_{ij}}(x_2) \quad (15)$$



Where  $k = 1, 2, \dots, 9$ ,  $i = 1, 2, 3$ , and  $j = 1, 2, 3$ . Each node in this layer represents firing strength of the rule.

Layer 3: Every node in this layer is also a fixed node and represented by  $N$ . This is also known as normalizing layer given as

$$\bar{w}_k = w_k / (w_1 + w_2 + \dots + w_9) \quad (16)$$

Where  $k = 1, 2, \dots, 9$ , and output of each node in this layer is called the normalized firing strength.

Layer 4: This is known as defuzzifying layer, and every node in this layer is adaptive. The nodes of this layer are represented by square shape, and the node function is given as

$$O_k = \bar{w}_k f_k = \bar{w}_k (p_k x_1 + q_k x_2 + r_k) \quad (17)$$

Where  $p_k$ ,  $q_k$ , and  $r_k$  are the consequence parameters.

Layer 5: This is a single node layer represented by summation. The output of this layer represents the summation of all input signals. The node function for this layer is given as

$$Y = \sum_{k=1}^9 \bar{w}_k f_k \quad (18)$$

The ANFIS structure described above is used to compute the step size parameters  $\mu(k)$ , which is used to find optimum weight vector for LMS algorithm.

Learning of premise ( $m_i$  and  $n_i$ ) and consequence parameters ( $p_k$ ,  $q_k$ , and  $r_k$ ) in ANFIS structure is carried out with the hybrid learning algorithm [28]. This uses least-square and gradient descent methods to find consequent and premise parameters, respectively. The ANFIS structure proposed here, uses forward pass and backward pass learning algorithm. Suppose that  $S$ ,  $S_1$ , and  $S_2$  represent total set of parameters, set of premise parameters, and set of consequent parameters, respectively; then in the forward pass,  $S_1$  is unchanged, and  $S_2$  is computed using least-square error algorithm. The forward pass presents the input vector and node output to it. It can be calculated layer by layer till the corresponding data are obtained, and process is repeated. Once all data have been obtained, the value of consequence parameter set  $S_2$  can be

obtained and it also computes error signal for each training pair. In the backward pass,  $S_2$  is unchanged, and parameters of  $S_1$  are computed using gradient descent algorithm such as back propagation.

The error signal computed above propagates from output toward input end. The gradient vector is found for each training data entry, and updating of input parameters is performed with gradient descent algorithm. The step size parameter  $\mu(k)$  computed from ANFIS structure is used in LMS method given in (11). This method is used to extract fundamental active power weights ( $w_{ap}$ ,  $w_{bp}$ , and  $w_{cp}$ ) corresponding to the load currents. The average weight ( $w_{pavg}$ ) of active power weights is calculated as

$$w_{pavg} = (w_{ap} + w_{bp} + w_{cp}) / 3. \quad (19)$$

This average weight ( $w_{pavg}$ ) is added with the output of dc bus PI controller ( $w_{pdc}$ ), and reference active power weight ( $w_p$ ) is calculated as

$$w_p = w_{pavg} + w_{pdc}. \quad (20)$$

Active power components of reference supply currents ( $i_{pa}^*$ ,  $i_{pb}^*$ , and  $i_{pc}^*$ ) are estimated from the reference active power weight ( $w_p$ ) and unit in-phase templates ( $u_{pa}$ ,  $u_{pb}$ , and  $u_{pc}$ ) as

$$i_{pa}^* = w_p u_{pa}, \quad i_{pb}^* = w_p u_{pb}, \quad \text{and} \quad i_{pc}^* = w_p u_{pc}. \quad (21)$$

These active power components of reference supply currents are used to calculate total reference supply currents.

### B. Estimation of Fundamental Reactive Power Component of Reference Supply Currents

Unit quadrature templates ( $u_{qa}$ ,  $u_{qb}$ , and  $u_{qc}$ ) of PCC voltages are calculated from unit in-phase templates ( $u_{pa}$ ,  $u_{pb}$ , and  $u_{pc}$ ) as

$$u_{qa} = -u_{pb} / \sqrt{3} + u_{pc} / \sqrt{3} \quad (22)$$

$$u_{qb} = \sqrt{3} u_{pa} / 2 + (u_{pb} - u_{pc}) / 2\sqrt{3} \quad (23)$$

$$u_{qc} = -\sqrt{3} u_{pa} / 2 + (u_{pb} - u_{pc}) / 2\sqrt{3}. \quad (24)$$



Another PI controller in control algorithm is used to regulate voltage at PCC. The input for PI controller is error ( $v_{te}$ ) between actual PCC voltage ( $V_i$ ) and its reference value ( $V_i^*$ ). The output for PI controller at  $k$ th sampling instant is given as

$$w_t(k) = w_t(k-1) + k_{pq}\{v_{te}(k) - v_{te}(k-1)\} + k_{iq}(v_{te}(k)) \quad (25)$$

where parameters  $w_t$ ,  $k_{pq}$ , and  $k_{iq}$  are the PI controller output, proportional, and integral gains for voltage regulation, respectively.

The weights ( $w_{aq}$ ,  $w_{bq}$ , and  $w_{cq}$ ) corresponding to fundamental reactive power component of load current are extracted by ANFIS-LMS algorithm using (11), and average magnitude ( $w_{qavg}$ ) is calculated as

$$w_{qavg} = (w_{aq} + w_{bq} + w_{cq})/3. \quad (26)$$

The output of ac bus PI controller ( $w_t$ ) is a leading quadrature power component, which is used to compensate voltage drop in supply side impedance and loading of the system. The reference reactive power weight ( $w_q$ ) is calculated as

$$w_q = w_t - w_{qavg}. \quad (27)$$

The reference fundamental reactive power components of supply currents ( $i_{qa}^*$ ,  $i_{qb}^*$ , and  $i_{qc}^*$ ) are estimated from the reference reactive power weight ( $w_q$ ) and unit quadrature templates as

$$i_{qa}^* = w_q u_{qa}, \quad i_{qb}^* = w_q u_{qb}, \quad \text{and} \quad i_{qc}^* = w_q u_{qc}. \quad (28)$$

The estimated active and reactive power components are added to generate total reference supply currents.

### C. Estimation of Reference Supply Currents and Generation of Switching Pulses

The summation of reference active and reactive power components of (21) and (28) are considered as reference currents ( $i_{sa}^*$ ,  $i_{sb}^*$ , and  $i_{sc}^*$ ). These reference currents are compared with the sensed supply currents ( $i_{sa}$ ,  $i_{sb}$ , and  $i_{sc}$ ), and current

errors ( $i_{sae}$ ,  $i_{sbe}$ , and  $i_{sce}$ ) are evaluated. These current errors are passed through pulse width modulation (PWM) current controller for the generation of switching pulses for three-phase VSC used as DSTATCOM.

## IV. SIMULATION RESULTS AND DISCUSSION

A simulation model of the system utilizing proposed ANFISLMS-based control calculation is created in MATLAB/Simulink condition utilizing SPS toolbox. Execution of the control calculation for a shunt compensator is checked for power factor revision (PFC) and voltage regulation modes under nonlinear load for fluctuating load condition, for example, unbalancing and load change. The execution of DSTATCOM under different working conditions are appeared in the accompanying area, and the point by point simulation parameters are given in Appendix-A.



Fig.5: Performance of compensator for PFC mode under varying nonlinear load.

### A. Performance of DSTATCOM in PFC Mode

Fig. 5 delineates the dynamic execution of the shunt compensator for PFC mode under unequal load condition. In this, the waveforms of PCC voltages (versus), supply currents ( $i_s$ ), load currents ( $i_{la}$ ,  $i_{lb}$ , and  $i_{lc}$ ), compensator currents ( $i_{Ca}$ ,  $i_{Cb}$ , and  $i_{Cc}$ ), and dc link voltage ( $v_{dc}$ ) are spoken to. An unbalancing is made in load current amid  $t = 0.74 - 0.8$  s, when phase "c" is detached. Amid load unbalancing, it is observed that the supply currents are sinusoidal and adjusted with decreased amplitude.

The voltage at dc link is directed and accomplishes reference estimation of 750V. After  $t=0.8$  s, phase "c" of load is reconnected, and it is observed that dc link voltage accomplishes its reference an incentive inside a cycle. Fig. 6 speaks to harmonic spectra for phase "an" of PCC voltage ( $v_{sa}$ ), supply current ( $i_{sa}$ ), and load current ( $i_{la}$ ) alongside their waveforms. Fig. 6(a)– (c) indicates 2.39%, 2.57%, and 26.66% total harmonic distortions (THDs) in phase "an" of PCC voltage ( $v_{sa}$ ), supply current ( $i_{sa}$ ), and load current ( $i_{la}$ ), separately. The DSTATCOM with the assistance of proposed control can accomplish 2.57% THD in supply current which exists in the point of confinement indicated by IEEE-519 standard, notwithstanding when load current THD is around 26.66%. Figs. 5 and 6 portray satisfactory execution of DSTATCOM with ANFIS-LMS-based control calculation under changing load condition in PFC mode.

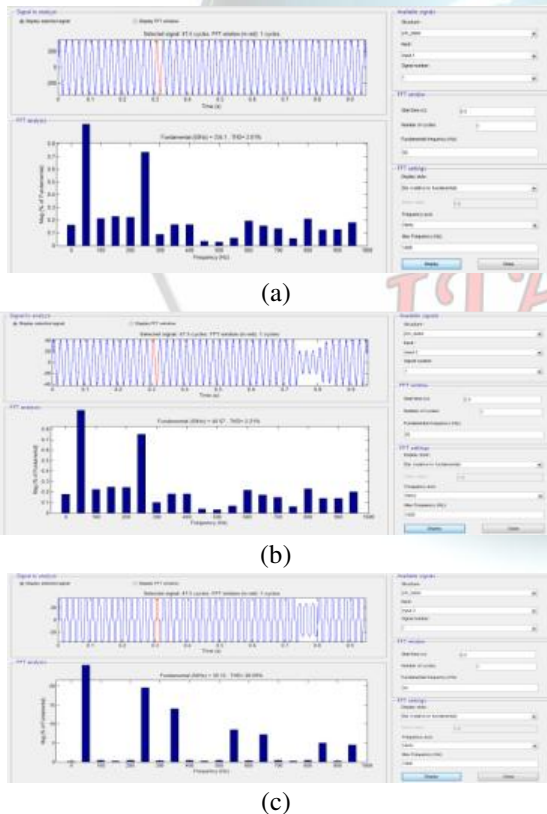


Fig.6: Harmonic spectra of phase "a" of (a) PCC voltage  $v_{sa}$ , (b) supply current  $i_{sa}$ , and (c) load current  $i_{la}$  in PFC mode.

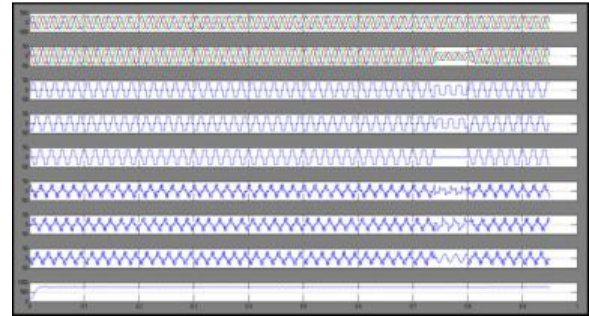


Fig.7: Performance of compensator for voltage regulation mode under varying nonlinear load.

### B. Performance of DSTATCOM in Voltage Regulation Mode

The reaction of shunt compensator for voltage regulation mode under fluctuating load condition is delineated in Fig. 7. In this figure, the waveforms of PCC voltages (versus), supply currents ( $i_s$ ), load currents ( $i_{la}$ ,  $i_{lb}$ , and  $i_{lc}$ ), compensator currents ( $i_{Ca}$ ,  $i_{Cb}$ , and  $i_{Cc}$ ), voltage at dc link ( $V_{dc}$ ), and size of PCC voltage ( $V_t$ ) are spoken to. An unbalancing in load is made amid  $t = 0.74 - 0.8$  s, when phase "c" of load is detached. Amid unbalancing, it is observed that supply currents are adjusted and sinusoidal. The size of PCC voltage is managed at reference estimation of 338.8 V. After  $t=0.8$  s, phase "c" of load is reconnected, and it is observed that PCC voltage accomplishes its reference esteem 338.8 V inside one cycle with the activity of PI controller.

Fig. 8(a)– (c) demonstrates harmonic spectra of phase "an" of PCC voltage ( $v_{sa}$ ), supply current ( $i_{sa}$ ), and load current ( $i_{la}$ ) alongside their waveforms, individually. These results portray 2.69%, 2.71%, and 26.83% THD in PCC voltage, supply current, and load current, separately. It is observed from these results that supply current accomplishes 2.71% THD, while there is 26.83%THD in load current. These results demonstrate the THDs of supply current and PCC voltage inside the cutoff determined by IEEE-519 standard. Figs. 7 and 8 portray satisfactory execution of DSTATCOM with ANFIS-LMS control calculation under shifting loads in voltage regulation mode.

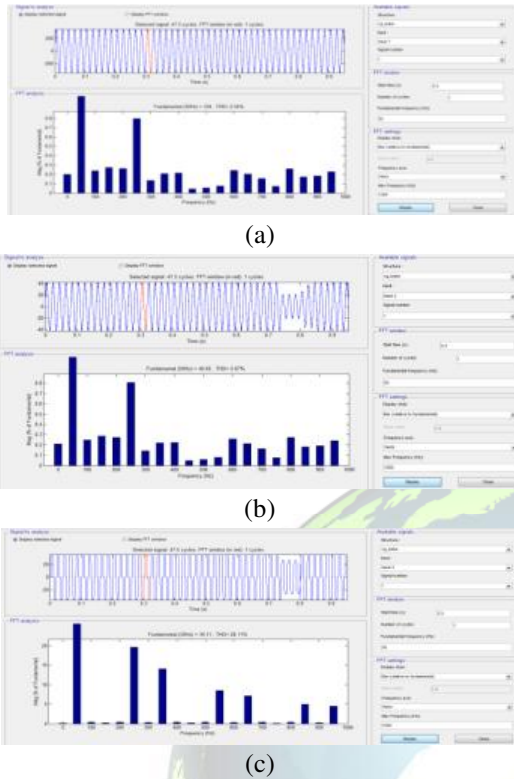


Fig.8: Waveforms and harmonic spectra of phase “a” of (a) PCC voltage  $v_{sa}$ , (b) supply current  $i_{sa}$ , and (c) load current  $i_{la}$  in voltage regulation mode.

### C. Comparative Performance of ANFIS-LMS-Based Control Algorithm

The proposed control calculation for DSTATCOM is contrasted and settled step LMS and VSLMS. Fig. 9 demonstrates the union of fundamental active power weight of load current for ANFIS-LMS-, LMS-, and VSLMS-based control calculations. It is observed from these results in Fig. 9 that the separated weight meets quicker and accomplishes constant incentive if there should arise an occurrence of ANFIS-LMS, while it wavers around the mean an incentive in the event of LMS and VSLMS control calculation. These are the execution of each of the three control calculations under load unbalancing. It is observed from these results that amid load unbalancing ( $t = 0.7 - 0.8$  s), an ANFIS-LMS calculation outputs a united weight with little wavering about the mean position. Be that as it may, the weights got with LMS and VSLMS calculations either don't unite or have

substantial motions. Because of managed and substantial motions in charge based on LMS and VSLMS, these calculations are less steady than ANFISLMS particularly under unequal load conditions. Fig. 10(a) and (b) demonstrates the harmonic spectra of supply current ( $i_{sa}$ ) with LMS- and VSLMS-based control calculations, separately. Supply current THDs of 4.29% and 3.62% are acquired with LMS and VSLMS, while supply current THD of 2.57% is gotten in ANFIS-LMS-based control for PFC mode. It might be closed from results appeared in Figs. 9(a) and (b) and 10(a) and (b) that the execution of ANFIS-LMS-based control calculation is better regarding joining and harmonic pay. The relative exhibitions of these control calculations are outlined in Table I.

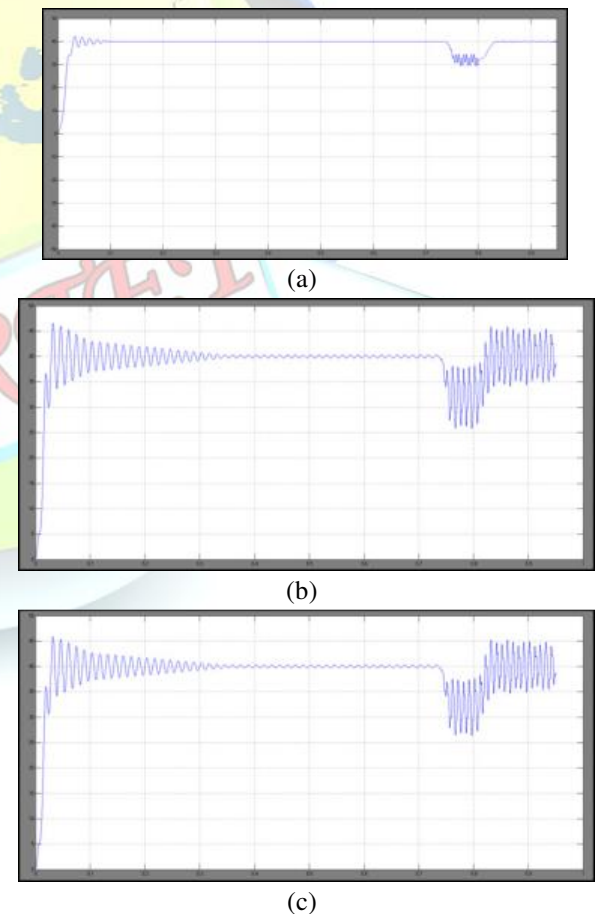


Fig.9: Comparative performance of weight convergence in unbalanced load conditions: (a) ANFIS-LMS (b) LMS (c) VSLMS.

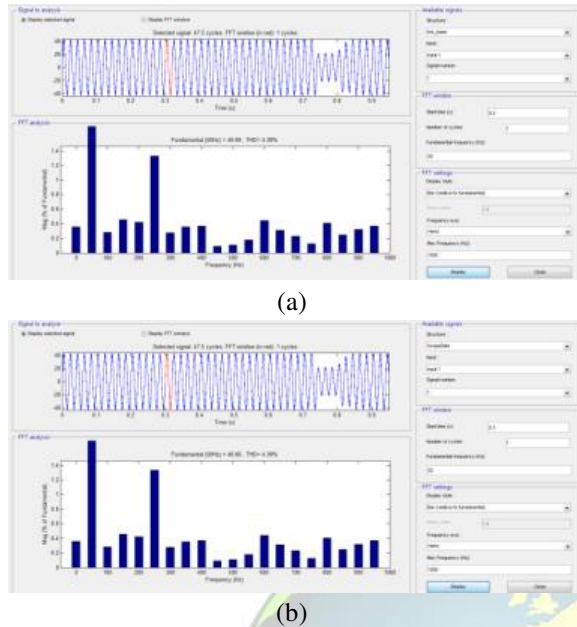


Fig.10: Harmonic spectra of (a) *isa* for LMS and (b) *isa* for VSLMS.

## VI. CONCLUSION

The ANFIS-LMS-based control calculation has been confirmed for the control of three-phase shunt compensator. This calculation has been utilized to extricate reference supply currents from nonsinusoidal load currents. The execution of DSTATCOM utilizing ANFIS-LMS-based control has been observed to be satisfactory for PFC and voltage regulation modes under changing load conditions. The power quality issues, for example, harmonics, reactive power, and load unbalancing have been moderated utilizing DSTATCOM. The THD in supply current has been decreased to 2.57% when there is THD of 26.66% in load current. The DSTATCOM has possessed the capacity to accomplish improved power quality, and after remuneration, the THD in supply currents lies inside the farthest point determined by IEEE-519 standard. The extents of voltages at PCC and dc bus have been managed to their reference esteems under steady-state and unbalancing load conditions. The ANFIS-LMS-based control calculation has been contrasted and settled step LMS and VSLMS control calculations. The proposed calculation has favorable circumstances over other two regarding quick

meeting, less static error, and quick learning of step size parameter.

## APPENDIX A

Rating of ac mains—415 V, three phase, and 50 Hz; source impedance  $R_s = 0.05 \Omega$ ,  $L_s = 1 \text{ mH}$ ; VSC rating 25 kVA; value of ripple filters  $R_f = 5 \Omega$ ,  $C_f = 5 \mu\text{F}$ ; value of interfacing inductor  $L_f = 3.4 \text{ mH}$ ; value of dc link capacitor  $C_{dc} = 1650 \mu\text{F}$ ; voltage at dc bus  $V_{dc} = 750 \text{ V}$ ; dc bus PI gains  $k_{pd} = 0.3$ ,  $k_{id} = 0.7$ ; gains of PI for voltage regulation  $k_{pq} = 0.015$ ,  $k_{iq} = 0.001$ ; three-phase uncontrolled diode rectifier with  $R = 15 \Omega$  and  $L = 100 \text{ mH}$ ; cutoff frequency of LPF used for dc bus voltage = 12 Hz; cutoff frequency of LPF used for PCC voltage magnitude = 10 Hz.

## REFERENCES

- [1] J. Schlabbach, D. Blume, and T. Stephanblome, *Voltage Quality in Electrical Power Systems*. Piscataway, NJ, USA: IEEE Press, 2001.
- [2] A. Ghosh and G. Ledwich, *Power Quality Enhancement Using Custom Power Devices*. New York, NY, USA: Springer, 2009.
- [3] B. Singh, A. Chandra, and K. Al-Haddad, *Power Quality: Problems and Mitigation Techniques*, Hoboken, NJ, USA: Wiley, 2015.
- [4] B. Singh, P. Jayaprakash, D. P. Kothari, A. Chandra, and K. Al Haddad, "Comprehensive study of DSTATCOM configurations," *IEEE Trans. Ind. Informat.*, vol. 10, no. 2, pp. 854–870, May 2014.
- [5] W. Shireena and T. Li, "A DSP-based active power filter for low voltage distribution systems," *Elect. Power Syst. Res.*, vol. 78, pp. 1561–1567, 2008.
- [6] C. Kumar and M. K. Mishra, "A multifunctional DSTATCOM operating under stiff source," *IEEE Trans. Ind. Electron.*, vol. 61, no. 7, pp. 3131–3136, Jul. 2014.
- [7] Christo Ananth, S. Esakki Rajavel, S. Allwin Devaraj, M. Suresh Chinnathampy. "RF and Microwave Engineering (Microwave Engineering).", ACES Publishers, Tirunelveli, India, ISBN: 978-81-910-747-5-8, Volume 1, June 2014, pp:1-300..
- [8] M. Popescu, A. Bitoleanu, and V. Suru, "A DSP-based implementation of the p–q theory in active



power filtering under nonideal voltage conditions,” *IEEE Trans. Ind. Informat.*, vol. 9, no. 2, pp. 880–889, May 2013.

[9] B. Singh and V. Verma, “Selective compensation of power-quality problems through active power filter by current decomposition,” *IEEE Trans. Power Del.*, vol. 23, no. 2, pp. 792–799, Apr. 2008.

[10] S. Bhattacharya, D. M. Divan, and B. Banerjee, “Synchronous frame harmonic isolator using active series filter,” in *Proc. Eur. Power Electron. (EPE’91)*, 1991, pp. 3030–3035.

[11] C. H. da Silva, R. R. Pereira, L. E. B. da Silva, G. Lambert-Torres, B. K. Bose, and S. U. Ahn, “A digital PLL scheme for three-phase system using modified synchronous reference frame,” *IEEE Trans. Ind. Electron.*, vol. 57, no. 11, pp. 3814–3821, Nov. 2010.

[12] S. Akhtar and D. S. Bernstein, “Lyapunov-stable discrete-time model reference adaptive control,” *Int. J. Adapt. Control Signal Process.*, vol. 19, pp. 745–767, 2005.

[13] V. Khadkikar, A. Chandra, and B.N. Singh, “Generalised single-phase p-q theory for active power filtering: simulation and DSP-based experimental investigation,” *IET Power Electron.*, vol. 2, no. 1, pp. 67–78, 2009.

[14] B. Singh and S. Arya, “Software PLL based control algorithm for power quality improvement in distribution system,” in *Proc. IEEE 5th India Int. Conf. Power Electron. (IICPE’12)*, 2012, pp. 1–6.

[15] M. Angulo, D. A. Ruiz-Caballero, J. Lago, M. L. Heldwein, and S. A. Mussa, “Active power filter control strategy with implicit closedloop current control and resonant controller,” *IEEE Trans. Ind. Electron.*, vol. 60, no. 7, pp. 2721–2730, Jul. 2013.

[16] B. Singh and J. Solanki, “An implementation of an adaptive control algorithm for a three-phase shunt active filter,” *IEEE Trans. Ind. Electron.*, vol. 56, no. 8, pp. 2811–2820, Aug. 2009.

[17] B. Singh and S. Arya, “Adaptive theory-based improved linear sinusoidal tracer control algorithm for DSTATCOM,” *IEEE Trans. Power Electron.*, vol. 28, no. 8, pp. 3768–3778, Aug. 2013.

[18] M. L. Jiangzi, “Application of adaptive filtering in harmonic analysis and detection,” in *Proc.*

*IEEE/PES Transmiss. Distrib. Conf. Exhib. Asia Pac.*, Dalian, China, 2005, pp. 1–4.

[19] H. Li, Z. Wu, and F. Liu, “A novel variable step-size adaptive harmonic detecting algorithm applied to active power filter,” in *Proc. IEEE Int. Conf. Ind. Technol. (ICIT’06)*, Mumbai, India, 2006, pp. 574–578.

[20] T. Aboulnasr and K. Mayyas, “A robust variable learning rate LMStype algorithm: analysis and simulations,” *IEEE Trans. Signal Process.*, vol. 45, no. 3, pp. 631–639, Mar. 1997.

[21] Y. Qu, W. Tan, Y. Dong, and Y. Yang, “Harmonic detection using fuzzy LMS algorithm for active power filter,” in *Proc. IEEE Int. Power Eng. Conf. (IPEC’07)*, Singapore, 2007, pp. 1065–1069.

[22] B. Farhang-Boroujeny, *Adaptive Filters: Theory and Applications*. Hoboken, NJ, USA: Wiley, 1998.

[23] S. Arya and B. Singh, “Neural network based conductance estimation control algorithm for shunt compensator,” *IEEE Trans. Ind. Informat.*, vol. 10, no. 1, pp. 569–577, Feb. 2014.

[24] M. Qasim and V. Khadkikar, “Application of artificial neural networks for shunt active power filter control,” *IEEE Trans. Ind. Informat.*, vol. 10, no. 3, pp. 1765–1774, Aug. 2014.

[25] R. L. de Araujo Ribeiro, C. C. de Azevedo, and R. M. de Sousa, “A robust adaptive control strategy of active power filters for power-factor correction, harmonic compensation, and balancing of nonlinear loads,” *IEEE Trans. Power Electron.*, vol. 27, no. 2, pp. 718–730, Feb. 2012.

[26] M. Singh and A. Chandra, “Real-time implementation of ANFIS control for renewable interfacing inverter in 3P4W distribution network,” *IEEE Trans. Ind. Electron.*, vol. 60, no. 1, pp. 121–128, Jan. 2013.

[27] J. S. R. Jang and C. T. Sun, “Neuro-fuzzy modeling and control,” *Proc. IEEE*, vol. 83, no. 3, pp. 378–406, Mar. 1995.

**Mrs. P Pavani** is currently pursuing M.Tech in Electrical Power System Tudi Narasimha Reddy institute of technology & sciences, Gudur, Bibinagar, Yadadribhongiri, Telangana., Affiliated to JNTU Hyderabad. He received Bachelor of technology Degree in Electrical and Electronics Engineering



ISSN 2394-3777 (Print)

ISSN 2394-3785 (Online)

Available online at [www.ijartet.com](http://www.ijartet.com)

*International Journal of Advanced Research Trends in Engineering and Technology (IJARTET)*

*Vol. 4, Issue 4, April 2017*

from JAWAHARLAL NEHRU INSTITUTE OF TECHNOLOGY, Affiliated to JNTU Hyderabad in 2014, and his field of interest includes power systems.

Email id: [paruchuri.pavani19@gmail.com](mailto:paruchuri.pavani19@gmail.com)

### **Mr. P NIRANJAN**

He is currently working as Assistant Professor in EEE DEPARTMENT with Tudi Narasimha Reddy institute of technology & sciences, Gudur, Bibinagar, Yadadribhongiri, Telangana., Affiliated to JNTU Hyderabad. Her interest subjects are Electrical measurements and instrumentation, Electrical power system.

Email id: [pniranjaneee@gmail.com](mailto:pniranjaneee@gmail.com)

